

# Altered Network Characteristics of Spike-Wave Discharges in Juvenile Myoclonic Epilepsy

Clinical EEG and Neuroscience  
2017, Vol. 48(2) 111–117  
© EEG and Clinical Neuroscience  
Society (ECNS) 2015  
Reprints and permissions:  
sagepub.com/journalsPermissions.nav  
DOI: 10.1177/1550059415621831  
journals.sagepub.com/home/eeg  


Chany Lee<sup>1</sup>, Chang-Hwan Im<sup>1</sup>, Yong Seo Koo<sup>2</sup>, Jung-Ah Lim<sup>3</sup>, Tae-Joon Kim<sup>3</sup>,  
Jung-Ick Byun<sup>3</sup>, Jun-Sang Sunwoo<sup>3</sup>, Jangsup Moon<sup>3</sup>, Dong Wook Kim<sup>4</sup>, Soon-Tae Lee<sup>3</sup>,  
Keun-Hwa Jung<sup>3</sup>, Kon Chu<sup>3</sup>, Sang-Kun Lee<sup>3</sup>, and Ki-Young Jung<sup>5,3</sup>

## Abstract

Epilepsy is a disease marked by hypersynchronous bursts of neuronal activity; therefore, identifying the network characteristics of the epileptic brain is important. Juvenile myoclonic epilepsy (JME) represents a common, idiopathic generalized epileptic syndrome, characterized by spike-and-wave discharge (SWD) electroencephalographic (EEG) waveforms. We compare herein the network properties of periods of SWD and baseline activity using graph theory. EEG data were obtained from 11 patients with JME. Functional cortical networks during SWD and baseline periods were estimated by calculating the coherence between all possible electrode pairs in the delta, theta, alpha, beta and gamma bands. Graph theoretical measures, including nodal degree, characteristic path length, clustering coefficient, and small-world index were then used to evaluate the characteristics of epileptic networks in JME. We also assessed short- and long-range connections between SWD and baseline networks. Compared to baseline, increased coherence was observed during SWD in all frequency bands. The nodal degree of the SWD network, particularly in the frontal region, was significantly higher compared to the baseline network. The clustering coefficient and small-world index were significantly lower in the theta and beta bands of the SWD versus baseline network, but the characteristic path length did not differ among networks. Long-range connections were increased during SWD, particularly between frontal and posterior brain regions. Our study suggests that SWD in JME is associated with increased local (particularly in frontal region) connectivity. Furthermore, the SWD network was associated with increased long-range connections, and reduced small-worldness, which may impair information processing during SWD.

## Keywords

idiopathic generalized epilepsy, juvenile myoclonic epilepsy, spike-wave discharge, functional connectivity, graph theory

Received May 4, 2015; accepted November 9, 2015.

## Introduction

The human brain is considered as a large-scale complex network, which is simultaneously segregated and integrated via specific patterns of connectivity.<sup>1,2</sup> A network that has locally well-connected clusters and efficient global connections is called small-world network.<sup>3</sup> This property can be observed in various networks such as electric power grid, spread of infection, and social network.<sup>4,5</sup> A normal human brain is of a small-world network as revealed by graph theory, which is a mathematical tool to quantify characteristics of network topology.<sup>1</sup> It has been reported that changes of efficiency, organization, or small-worldness of the brain network occur in various neurological and psychiatric disorders.<sup>2,6,7</sup> Therefore, graph measures are probable markers of disease and can contribute to our understanding of how pathological processes lead to neurological impairments.<sup>8</sup>

<sup>1</sup>Department of Biomedical Engineering, Hanyang University, Seoul, Korea

<sup>2</sup>Department of Neurology, Korea University Medical Center, Korea University College of Medicine, Seoul, Korea

<sup>3</sup>Department of Neurology, Laboratory for Neurotherapeutics, Comprehensive Epilepsy Center, Biomedical Research Institute, Seoul National University Hospital, Seoul, Korea

<sup>4</sup>Department of Neurology, Konkuk University School of Medicine, Seoul, Korea

<sup>5</sup>Department of Neurology, Seoul National University Hospital, Neuroscience Research Institute, Seoul National University College of Medicine, Seoul, Korea

### Corresponding Author:

Ki-Young Jung, Department of Neurology, Seoul National University Hospital, Neuroscience Research Institute, Seoul National University College of Medicine, Seoul, Korea, #103, Daehak-ro, Jongno-Gu, Seoul 110-799, Korea.

Email: jungky@snu.ac.kr

Full-color figures are available online at journals.sagepub.com/home/eeg

Epilepsy is a disease of functionally and/or structurally aberrant connections between neurons and groups of neurons at the systems level.<sup>9</sup> The initiation of seizures or ictogenesis is emergent properties of aberrant neuronal connections. In partial epilepsy, it has been well known that synchrony increases on the smallest and largest spatial scales in the beginning of focal seizure.<sup>10</sup> Therefore, during epileptic seizures, hypercorrelated and functionally segregated brain areas are reintegrated into more collective brain dynamics.<sup>10</sup> Similar to this, the functional neural network changes during generalized seizures. Altered thalamo-cortical network in idiopathic generalized epilepsy (IGE) has been implicated as an underlying pathophysiological mechanism.<sup>11-14</sup> Cortico-cortical network is also important for initiation and propagation of spike-and-wave discharge.<sup>14-17</sup> Therefore, generalized seizures have cortical onset and the thalamus has an essential role in the recruitment of a network comprising frontal, parietal and occipital cortex and the default mode network. Furthermore, unlike in partial epilepsy, it has been reported that preexisting functional and anatomical networks that normally serve highly important physiological functions take part in the ictogenic mechanisms in IGEs.<sup>18</sup>

Juvenile myoclonic epilepsy (JME), which represents the most common idiopathic IGE syndrome,<sup>19,20</sup> is characterized by myoclonic jerks on awakening, generalized tonic-clonic seizures, and less frequent absence seizures. On EEG, JME typically consists of bilateral, synchronous, widespread spikes, or polyspikes, and wave complexes (known as spike-and-wave discharges or SWDs), which are commonly assumed to occur without lateralization or localization.<sup>21</sup> In the previous study, we reported the ictogenesis are initiated in the precuneus and sustained by a network involving the frontal cortex, precuneus, and thalamus in JME. However, it remains unclear how these brain regions are organized, and tell us little about the underlying mechanism that drives these changes in connectivity. Although increased functional connectivity in the delta band has been reported during the baseline state in patients with JME,<sup>15</sup> no study has investigated network topology during the ictal state in this population.

We compared herein the characteristics of SWD network topology and baseline networks in JME patients, with the aim of further elucidating the mechanisms underlying SWD. First, we evaluated nodal degree, because it has been frequently reported that local network properties are important in generalized epilepsy.<sup>3</sup> Second, graph theoretical measures, including clustering coefficient (Cp), characteristic path length (Lp) and small-worldness, were evaluated in different frequency bands. Cp and Lp are related to local and global efficiency of network, respectively.<sup>22</sup> Third, the regional connectivity of the 2 different states was estimated and compared.

## Methods

### Subjects

Eleven patients with a clinical diagnosis of JME were included; the diagnosis was based on the electroclinical criteria of the International League Against Epilepsy.<sup>23</sup> The inclusion criteria

were as follows: (1) typical clinical history of JME with onset of myoclonic jerks and generalized seizures in adolescence, (2) no evidence of neurological abnormality and intellectual decline, (3) apparent spike (or polyspike) and wave discharges on a normal background rhythm on the previously standard international 10-20 EEG system, and (4) normal MRI findings on visual inspection. The study protocol was approved by the local ethical committee.

### EEG Recording

Routine waking and sleep EEG recordings were recorded from each patient, for approximately 1 hour, using a 64-channel digital EEG machine (Grass Technologies, Quincy, MA, USA). An electrode cap with sintered Ag/AgCl electrodes (Quick-Cap, Compumedics Neuroscan, Charlotte, NC, USA) was used and impedance was maintained below 10 kohm. An average mastoid reference was employed. The sampling rate was 1600 Hz, and the bandpass filter was set at 0.3 to 70 Hz.

### Selection of SWD and Interictal EEG

An epilepsy specialist (KJ) visually inspected whole EEG recordings and selected epochs. All SWDs were bilateral and widespread at a frequency of 2 to 5 Hz. The onset of SWD was defined as the first large transition in SWD signals.<sup>20</sup> Epochs of SWD were extracted from -100 to 900 ms, and the spike onset time was 0 ms. One-second baseline epochs with no abnormalities were selected during waking and resting states while patients closed their eyes. The number of epochs selected is listed in Table 1.

### Connectivity and Graph Theoretical Analysis

A graph is a set of nodes and links.<sup>4</sup> In the present research, electrodes corresponded nodes and a link between two nodes was defined by calculating functional connectivity between EEG signals of two electrodes. Functional connectivity during SWD and baseline periods was evaluated by coherence, which reflects a level of functional signal communication between different areas of the brain.<sup>24</sup> To avoid potential volume conduction effects,<sup>25</sup> coherence was computed after applying the surface Laplacian using the CSD Toolbox.<sup>26,27</sup> Coherence values of all possible electrode pairs were then calculated for delta (0-4 Hz), theta (4-8 Hz), alpha (8-13 Hz), beta (13-30 Hz), and gamma (30-50 Hz) bands. To construct undirected and unweighted graphs, electrode pairs with upper 10% coherence values were selected to represent the links of the graphs, such that the mean nodal degree was approximately  $K = 6$ .

In the present study, nodal degree, Cp, Lp, and small-world index (SWI) were used for graph measures. Nodal degree is the number of links incident to the other vertices, so a region with high nodal degree could be a hub of the network.<sup>4</sup> If neighbors of a given node were also neighbors of each other, they were considered to be a cluster. Cp can be obtained by averaging fraction of clusters in the graph and this measure represents local efficiency of information transfer of a network.<sup>28</sup> Lp which is the mean shortest path between possible node-pairs has reciprocal relationship to global efficiency of the network.<sup>28,29</sup> For significance of

**Table 1.** Clinical Characteristics of Patients.

Patient No.	Sex	Age (Years)	Onset (Years)	No. of Epoch	AEDs
1	Male	42	13	6	LMT, VPA
2	Male	19	16	12	LEV
3	Female	24	22	32	LEV
4	Male	19	16	7	VPA
5	Male	24	18	14	LEV
6	Male	32	30	21	ZNS
7	Female	17	12	6	VPA, LEV
8	Male	19	19	4	VPA
9	Male	13	12	4	LEV, VPA
10	Male	28	10	25	LEV, OXC
11	Female	24	11	10	LEV
Mean		24.8	16.7	12.8	
SD		7.6	6.0	9.4	

Abbreviations: AED, antiepileptic drug; LEV, levetiracetam; LMT, lamotrigine; OXC, oxcarbazepine; VPA, valproate; ZNS, zonisamide.

Cp and Lp compared to random network, we created 100 surrogate random networks with an identical nodal degree, and normalized Cp and Lp.<sup>5</sup> Then, we yielded SWI defined as the proportion of Cp to Lp.<sup>1</sup> A network can be called small-world if SWI is larger than 1, and high SWI network is well-balanced between local processing and global integration.<sup>4</sup> Degree, Cp, and Lp were calculated using the Brain Connectivity Toolbox.<sup>1</sup>

Coherence was divided into short- and long-range connections, in terms of distance between electrodes.<sup>30</sup> A short-range connection was defined as coherence between an electrode and any adjacent electrode no more than 2 steps apart; all other connections were defined as long-range.

To investigate regional connectivity, six scalp regions were distinguished as follows: frontal (F3, F1, Fz, F2, F4), central (C3, C1, Cz, C2, C4), parietal (P3, P1, Pz, P2, P4), occipital (O1, Oz, O2), left temporal (FT7, T7, Tp7) and right temporal (FT8, T8, TP8) regions. The number of connections between 2 subregions was normalized by the number of all possible connections between them.

### Statistical Analysis

The Wilcoxon signed-rank sum test was used to assess differences between graph theoretical measures (coherence, nodal degree, Cp, Lp and SWI), because the Kolmogorov-Smirnov test indicated that no measures were normally distributed.<sup>31</sup> A value of  $P = .05$  was taken to indicate statistical significance. All analyses were performed using the MatLab 7.1 (MathWorks, Natick, MA, USA).

## Results

### Patients and EEG Characteristics

Patients' clinical and EEG data are summarized in Table 1. All patients showed good seizure outcomes with 1 or 2 antiepileptic drugs (AEDs) administered. Valproate and levetiracetam were the most commonly prescribed AEDs. Epochs were selected

from the EEG in 2- to 5-Hz SWDs. Among patients, the number of epochs ranged between 4 and 32 (mean  $12.8 \pm 9.4$ ).

### Nodal Degree

The nodal degree of the SWD network, at each coherence value, was significantly higher for all frequency bands compared with the baseline network (Figure 1). The topographic distribution of the nodal degree indicated that it was significantly higher in frontal regions, at all frequency bands in the SWD versus baseline network (Figure 2). This frontal nodal degree prominence was more evident in lower frequency bands, such as the delta and theta bands.

### Clustering Coefficient, Characteristic Path Length, and Small-World Index

The Cp values of the SWD network were significantly lower compared with those of the baseline network, in the theta and beta bands, whereas Lp did not differ among networks. Consequently, SWI values in the theta and beta bands were significantly lower during the SWD versus baseline period (Figure 3).

A representative example (patient 7) of topographic distributions, in the theta band of the baseline and SWD networks, is shown in Figure 4. In the baseline period, the network consisted primarily of short-range connections and small-size clusters, whereas in the SWD network there were few short-range connections and clusters but an increased number of long-range connections, particularly between frontal and parietal regions.

In the SWD network, the frontal region exhibited the highest degree of connectivity with other scalp regions. The normalized number of connections between frontal and other subregions in the theta and beta bands is shown in Figure 5. The normalized number of connection was increased in all tested regions and more patients showed increased regional connectivity with frontal region of SWD network except right temporal region in theta band. Especially, connectivity between frontal and parietal regions did not decrease any of the patients.

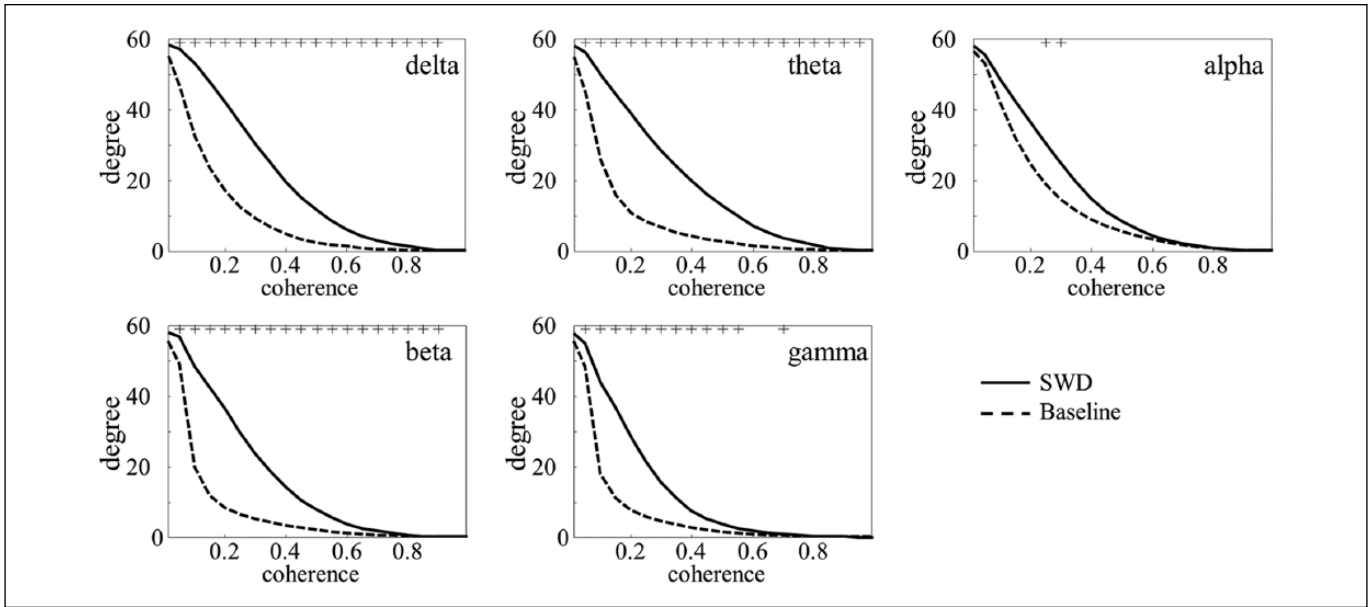


**Figure 1.** Mean coherence values in accordance with coherence threshold. In all bands, values during spike-and-wave discharge (SWD) are higher versus baseline. “+” indicates statistical significance.

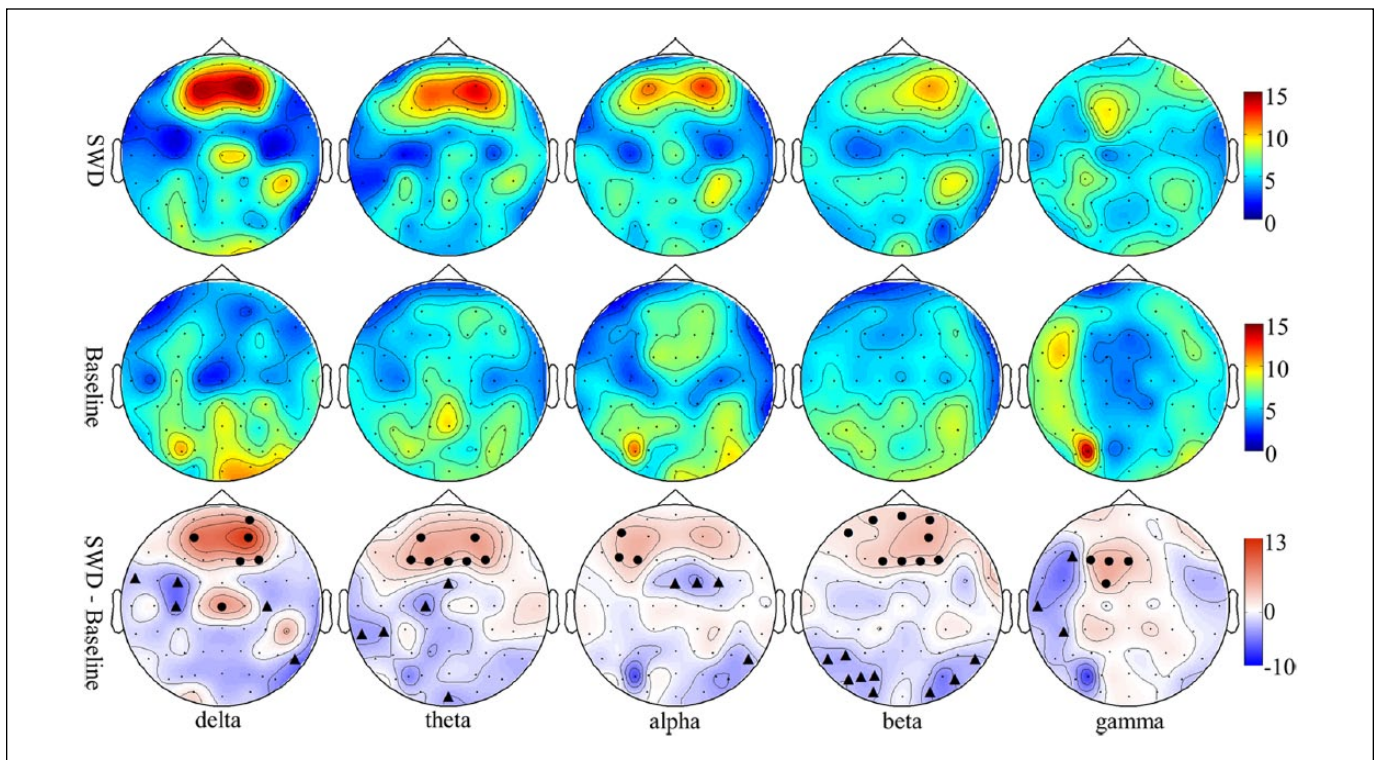


**Figure 2.** Averaged nodal degree distributions during spike-and-wave discharge (SWD) (top), baseline (middle) periods, and the difference between the two periods (bottom). While the SWD network is characterized by a significantly higher nodal degree in frontal regions compared to baseline (denoted by •), the baseline network has a significantly higher nodal degree in central and posterior regions (denoted by ▲). The colored section represents the averaged nodal degree.

**Discussion**

We investigated differences in the topology of functional networks, during SWD and baseline periods, in patients with JME using graph theory. Our main findings were as follows: the

SWD network, in comparison with the baseline state, was characterized by (1) increased nodal degree in frontal regions; (2) a smaller clustering coefficient, but with no change in characteristic path length resulting in a decreased SWI; and (3) a reduced

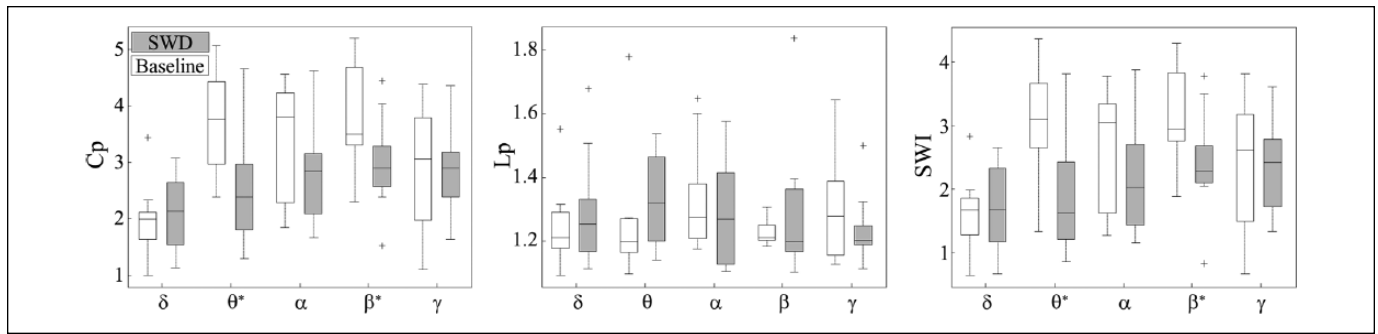


**Figure 3.** Clustering coefficient ( $C_p$ ), characteristic path length ( $L_p$ ), and small-world index (SWI) of the spike-and-wave discharge (SWD) and baseline periods. In the theta and beta bands, the  $C_p$  and SWI of SWD are smaller versus baseline. However,  $L_p$  does not differ between periods.

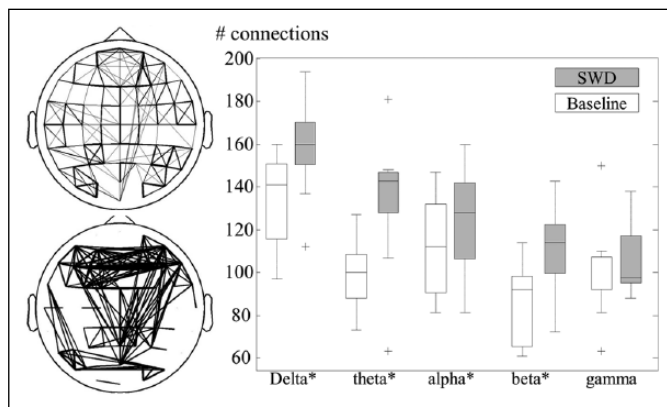


**Figure 4.** Increased long-range connectivity in spike-and-wave discharge (SWD). The upper and lower left panels show the baseline and SWD networks, respectively, of patient 7 in the theta frequency. The networks exhibit an identical mean nodal degree ( $K = 6$ ). Change in long-range connectivity is shown in right panel. The number of long-range connections is significantly increased in the delta, theta, alpha and beta bands.

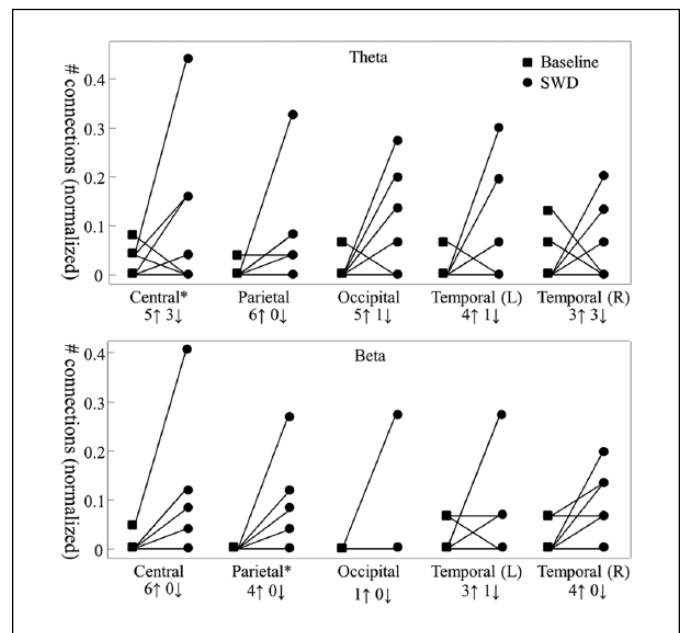


**Figure 5.** Change in the density of the connection to the frontal region in the theta (upper panel) and beta (lower panel) bands. Each line corresponds to a different patient. On the x-axis, the numbers before the upward- and downward-pointing arrows correspond to the numbers of patients with increased and decreased connections to the frontal region. The y-axis denotes the normalized number of connections to the frontal region.

number of short-range, and increased number of long-range connections, mainly between frontal and posterior regions.

The overall increase in nodal degree in the SWD versus baseline network, at an identical threshold level of coherence, indicates that average coherence increased during SWD. This accords with previous reports indicating that SWD reflects increased synchronization.<sup>3,21</sup> The involvement of frontal region during SWD, in patients with IGE, including JME, has also been reported frequently. During SWD periods in JME patients, EEG activity predominantly occurs in the fronto-central area.<sup>32,33</sup> EEG and MEG studies also indicate that frontal region possess a current source during SWD;<sup>20,34</sup> furthermore, frontal deactivation of the BOLD (blood oxygen level-dependent) signal has been observed after SWD onset.<sup>35</sup>

In addition to local behavior in the frontal region, its connectivity with other regions is also important to understand the pathophysiology of SWD. In our study, frontal nodal connectivity was significantly increased in the SWD network, mainly attributable to long-range connections between frontal and

posterior brain regions. This fronto-parietal connection is important for attentional network, and cognitive impairments of patients with IGE were reported in previous studies.<sup>36,37</sup> Hence, abnormality of fronto-parietal connection during SWD may interfere with proper function of attentional system.

While the clustering coefficient of the SWD network was significantly lower compared to the baseline network, in the theta and beta bands, characteristic path length did not differ among networks, which may explain the decreased SWI values in the theta and beta bands. A smaller clustering coefficient in the SWD network results from reduced local connectivity compared with baseline. In contrast, the characteristic path length, indicative of

global connections, did not differ significantly between the baseline and SWD. As shown in Figure 4, many nodes were connected to adjacent nodes during the baseline period, such that network was characterized by a high number of small-sized clusters. During SWD, long-range connectivity was enhanced, and small clusters were dissolved; therefore, connections between frontal and other subregions were increased (Figure 5). In particular, connections between frontal and parietal regions in the theta band were significantly increased, supporting the involvement of the parietal region in IGE.<sup>35,38</sup>

The lowered SWI that we observed suggest that epileptic signals are transferred across distant regions directly, instead of via well-organized and small-world functional networks, which results in less efficient information processing during SWD. Numerous reports indicated that patients with IGE, including absence epilepsy and JME, exhibit a degree of cognitive impairment.<sup>36,37</sup> Neuropsychological testing has revealed subtle dysfunctions in several cognitive domains, including frontal executive and nonverbal memory function.<sup>39</sup> These cognitive impairments have been corroborated by imaging studies indicating reductions in gray matter volume in the supplementary motor area and posterior cingulate cortex, and reductions in fractional anisotropy in the underlying white matter of the corpus callosum.<sup>39,40</sup>

Increased relative theta power in patients with IGE has been reported,<sup>41</sup> and theta band power and coherence may indicate theta oscillation in the thalamo-cortical network,<sup>42</sup> a key component of IGE pathophysiology.<sup>20,43</sup> Therefore, our data supports the notion that theta and beta band connectivity might play an important role in the JME network.

Our study had several limitations. First, only a small number of patients were included; further studies including a larger number of subjects are required to validate our results. Second, all patients were taking AEDs, which may have affected brain oscillation and networks. Furthermore, connectivity among cortical current sources was not considered. We adopted a surface Laplacian approach to reduce volume current effects, but EEG signals are not entirely reflective of neuronal activity occurring underneath the electrode.<sup>44</sup> Previous studies have employed source-level connectivity analysis.<sup>45,46</sup> However, this approach can result in the acquisition of different source distributions, because inverse algorithms are selected by the researcher. Multiple sources may be problematic because connectivity is typically calculated using pairwise or multivariate analyses. One of other limitation is related to time resolution: SWD represents a dynamic state, but we used coherence to estimate connectivity during a single second. Good time resolution represents a particular advantage of EEG; therefore, it is important to employ a suitable connectivity measure. A final limitation of this study is inconsistent results of graph theoretical analysis on epilepsy. According to the article of Kramer and Cash,<sup>47</sup> connectivity and graph theoretical measures of researches on epilepsy cannot show identical results. We expect that elaborate analysis will show more helpful information about underlying mechanism of epilepsy.

## Conclusion

We compared herein the connectivity and network characteristics of baseline and SWD periods in patients with JME, and observed increased functional connectivity during SWD, particularly in the frontal region. SWD networks were associated with increased long-range connectivity, particularly between frontal and posterior brain regions, and decreased small-worldness that impaired the efficiency of information processing during SWD.

## Author Contributions

CL contributed to analysis and interpretation of data and drafting manuscript. C-HI contributed to conception and critical revision. YSK contributed to design and acquisition of data. J-AL, T-JK, J-IB, J-SS, and JM contributed to conception and interpretation of data. DWK, S-TL, K-HJ, KC, and S-KL contributed to critical revision. K-YJ contributed to conception, interpretation of data, drafting manuscript and critical revision.

## Declaration of Conflicting Interests

The author(s) declared no conflicts of interest with respect to the research, authorship, and/or publication of this article.

## Funding

The author(s) disclosed receipt of the following financial support for the research, authorship, and/or publication of this article: This research was supported by Basic Science Research Program through the National Research Foundation of Korea (NRF) funded by the Ministry of Science, ICT & Future Planning (NRF-2014R1A2A2A04003858), and Bio & Medical Technology Development Program of the National Research Foundation (NRF) funded by the Ministry of Science, ICT & Future Planning (NRF-2011-0027860).

## References

1. Rubinov M, Sporns O. Complex network measures of brain connectivity: uses and interpretations. *Neuroimage*. 2010;52:1059-1069.
2. Shim M, Kim DW, Lee SH, Im CH. Disruptions in small-world cortical functional connectivity network during an auditory odd-ball paradigm task in patients with schizophrenia. *Schizophr Res*. 2014;156:197-203.
3. Gupta D, Ossenblok P, van Luijtelaar G. Space-time network connectivity and cortical activations preceding spike wave discharges in human absence epilepsy: a MEG study. *Med Biol Eng Comput*. 2011;49:555-565.
4. Stam CJ, Reijneveld JC. Graph theoretical analysis of complex networks in the brain. *Nonlinear Biomed Phys*. 2007;1:3.
5. Watts DJ, Strogatz SH. Collective dynamics of "small-world" networks. *Nature*. 1998;393:440-442.
6. Ahmadlou M, Adeli H, Adeli A. Graph theoretical analysis of organization of functional brain networks in ADHD. *Clin EEG Neurosci*. 2012;43:5-13.
7. Liu T, Chen Y, Lin P, Wang J. Small-world brain functional networks in children with attention-deficit/hyperactivity disorder revealed by EEG synchrony. *Clin EEG Neurosci*. 2015;46:183-191.

8. Petrella JR. Use of graph theory to evaluate brain networks: a clinical tool for a small world? *Radiology*. 2011;259:317-320.
9. Engel J, Thompson PM, Stern JM, Staba RJ, Bragin A, Mody I. Connectomics and epilepsy. *Curr Opin Neurol*. 2013;26:186-194.
10. Rummel C, Goodfellow M, Gast H, et al. A systems-level approach to human epileptic seizures. *Neuroinformatics*. 2013;11:159-173.
11. Tyvaert L, Chassagnon S, Sadikot A, LeVan P. Thalamic nuclei activity in idiopathic generalized epilepsy: an EEG-fMRI study. *Neurology*. 2009;73:2018-2022.
12. Gotman J, Grova C, Bagshaw A, Kobayashi E, Aghakhani Y, Dubeau F. Generalized epileptic discharges show thalamocortical activation and suspension of the default state of the brain. *Proc Natl Acad Sci U S A*. 2005;102:15236-15240.
13. Moeller F, Siebner HR, Wolff S, et al. Changes in activity of striato-thalamo-cortical network precede generalized spike wave discharges. *Neuroimage*. 2008;39:1839-1849.
14. Meeren H, Pijn J, Van Luijtelaar E, Coenen A, Lopes da Silva F. Cortical focus drives widespread corticothalamic networks during spontaneous absence seizures in rats. *J Neurosci*. 2002;22:1480-1495.
15. Clemens B, Puskás S, Besenyei M, et al. Neurophysiology of juvenile myoclonic epilepsy: EEG-based network and graph analysis of the interictal and immediate preictal states. *Epilepsy Res*. 2013;106:357-369.
16. Meeren H, van Luijtelaar G, Lopes da Silva F, Coenen A. Evolving concepts on the pathophysiology of absence seizures: the cortical focus theory. *Arch Neurol*. 2005;62:371-376.
17. Lin K, Jackowski AP, Carrete H Jr, et al. Voxel-based morphometry evaluation of patients with photosensitive juvenile myoclonic epilepsy. *Epilepsy Res*. 2009;86:138-145.
18. Wolf P, Beniczky S. Understanding ictogenesis in generalized epilepsies. *Expert Rev Neurother*. 2014;14:787-798.
19. Vollmar C, O'Muircheartaigh J, Barker GJ, et al. Motor system hyperconnectivity in juvenile myoclonic epilepsy: a cognitive functional magnetic resonance imaging study. *Brain*. 2011;134 (pt 6):1710-1719.
20. Lee C, Kim S-M, Jung Y-J, Im C-H, Kim DW, Jung K-Y. Causal influence of epileptic network during spike-and-wave discharge in juvenile myoclonic epilepsy. *Epilepsy Res*. 2014;108:257-266.
21. Nordli DR Jr. Idiopathic generalized epilepsies recognized by the International League Against Epilepsy. *Epilepsia*. 2005;46(suppl 9):48-56.
22. Bassett DS, Bullmore E. Small-world brain networks. *Neuroscientist*. 2006;12:512-523.
23. Commission of International League Against Epilepsy. Proposal for revised classification of epilepsies and epileptic syndromes. *Epilepsia*. 1989;30:389-399.
24. Thatcher RW, Krause PJ, Hrybyk M. Cortico-cortical associations and EEG coherence: a two-compartmental model. *Electroencephalogr Clin Neurophysiol*. 1986;64:123-143.
25. Srinivasan R, Winter WR, Ding J, Nunez PL. EEG and MEG coherence: measures of functional connectivity at distinct spatial scales of neocortical dynamics. *J Neurosci Methods*. 2007;166:41-52.
26. Kayser J, Tenke CE. Principal components analysis of Laplacian waveforms as a generic method for identifying ERP generator patterns: I. Evaluation with auditory oddball tasks. *Clin Neurophysiol*. 2006;117:348-368.
27. Kayser J, Tenke CE. Principal components analysis of Laplacian waveforms as a generic method for identifying ERP generator patterns: II. Adequacy of low-density estimates. *Clin Neurophysiol*. 2006;117:369-380.
28. He Y, Evans A. Graph theoretical modeling of brain connectivity. *Curr Opin Neurol*. 2010;23:341-350.
29. Bullmore E, Sporns O. Complex brain networks: graph theoretical analysis of structural and functional systems. *Nat Rev Neurosci*. 2009;10:186-198.
30. Weiss S, Rappelsberger P. Long-range EEG synchronization during word encoding correlates with successful memory performance. *Cogn Brain Res*. 2000;9:299-312.
31. Hornero R, Abásolo D, Escudero J, Gómez C. Nonlinear analysis of electroencephalogram and magnetoencephalogram recordings in patients with Alzheimer's disease. *Philos Trans A Math Phys Eng Sci*. 2009;367:317-336.
32. Anderson J, Hamandi K. Understanding juvenile myoclonic epilepsy: contributions from neuroimaging. *Epilepsy Res*. 2011;53:779-789.
33. Serafini A, Rubboli G, Gigli GL, Koutroumanidis M, Gelisse P. Neurophysiology of juvenile myoclonic epilepsy. *Epilepsy Behav*. 2013;28(suppl 1):S30-S39.
34. Westmijse I, Ossenblok P, Gunning B, van Luijtelaar G. Onset and propagation of spike and slow wave discharges in human absence epilepsy: a MEG study. *Epilepsia*. 2009;50:2538-2548.
35. Benuzzi F, Mirandola L, Pugnaghi M, et al. Increased cortical BOLD signal anticipates generalized spike and wave discharges in adolescents and adults with idiopathic generalized epilepsies. *Epilepsia*. 2012;53:622-630.
36. Blumenfeld H. Consciousness and epilepsy: why are patients with absence seizures absent? *Prog Brain Res*. 2005;150:271-286.
37. Killory BD, Bai X, Negishi M, et al. Impaired attention and network connectivity in childhood absence epilepsy. *Neuroimage*. 2011;56:2209-2217.
38. Vaudano AE, Laufs H, Kiebel SJ, et al. Causal hierarchy within the thalamo-cortical network in spike and wave discharges. *PLoS One*. 2009;4:e6475.
39. O'Muircheartaigh J, Vollmar C, Barker GJ, et al. Focal structural changes and cognitive dysfunction in juvenile myoclonic epilepsy. *Neurology*. 2011;76:34-40.
40. Kim JH, Suh S-I, Park S-Y, et al. Microstructural white matter abnormality and frontal cognitive dysfunctions in juvenile myoclonic epilepsy. *Epilepsia*. 2012;53:1371-1378.
41. Clemens B, Szigeti G, Barta Z. EEG frequency profiles of idiopathic generalised epilepsy syndromes. *Epilepsy Res*. 2000;42:105-115.
42. Clemens B. Pathological theta oscillations in idiopathic generalised epilepsy. *Clin Neurophysiol*. 2004;115:1436-1441.
43. Stefan H, Paulini-Ruf A, Hopfengärtner R, Rampp S. Network characteristics of idiopathic generalized epilepsies in combined MEG/EEG. *Epilepsy Res*. 2009;85:187-198.
44. Nunez PL, Srinivasan R, Westdorp AF, et al. EEG coherence. I: statistics, reference electrode, volume conduction, Laplacians, cortical imaging, and interpretation at multiple scales. *Electroencephalogr Clin Neurophysiol*. 1997;103:499-515.
45. Wilke C, Worrell G, He B. Graph analysis of epileptogenic networks in human partial epilepsy. *Epilepsia*. 2011;52:84-93.
46. O'Muircheartaigh J, Vollmar C, Barker GJ, et al. Abnormal thalamocortical structural and functional connectivity in juvenile myoclonic epilepsy. *Brain*. 2012;135(pt 12):3635-3644.
47. Kramer MA, Cash SS. Epilepsy as a disorder of cortical network organization. *Neuroscientist*. 2012;18:360-372.